CIMAC CONGRESS 25
ZURICH, MAY 19 – 23, 2025

2025 | 178

Experimental Long-Term Study of a Methane Oxidation Catalyst on a Medium-Speed Dual-Fuel Engine

Exhaust Gas Aftertreatment Solutions & CCS

Pascal Seipel, University of Rostock

Manuel Glauner, University of Rostock
Sebastian Cepelak, University of Rostock
Jules Christopher Dinwoodie, University of Rostock
Karsten Schleef, University of Rostock
Bert Buchholz, University of Rostock
Robert Bank, FVTR Rostock

DOI: https://doi.org/10.5281/zenodo.15191505

ABSTRACT

The dual-fuel combustion process, which is offered as a retrofit solution for conventional diesel engines by various manufacturers represents an option for reducing emissions from internal combustion engines and is already available today. Current dual-fuel engines run on liquefied natural gas (LNG), which is usually of fossil origin. Thanks to the existing infrastructure and the possibility of producing LNG by means of electrolysis and methanation, LNG can already be produced in a 100 % climate-neutral way and thus make a contribution to climate neutrality in the shipping industry.

A central issue in the TEME2030+ project is the investigation and reduction of the methane slip that exists in dual-fuel engines. Methane slip is the result of the valve overlap in turbo-charged gas engines with port fuel injection and of incomplete combustion processes within the cylinder. The escaped gas significantly reduces the emission advantages of dual-fuel engines due to methane's high greenhouse gas potential of 29.8, making the reduction of methane emissions a critical point in the development of future dual-fuel engines.

One way to reduce methane emissions is to use methane oxidation catalysts (MOC), which can be divided into two groups: precious metal-containing and precious metal-free catalysts. The advantage of catalytic converters containing precious metals, such as catalytic converters with a palladium coating, is the lower light-off temperature, which makes them suitable for dual-fuel engines without external heating. These converters are, however, known to have a short life span, due to the high water content of exhaust gas in the case of fuels with high H to C ratios (like methane) and potentially due to sulphur dioxide contained in the exhaust gas. The investigation of the conversion rate with the addition of various test gases on the synthesis gas test bench and tests on the single-cylinder engine are important for assessing the potential.

The following paper describes the behaviour of a precious metal-containing MOC with a palladium coating on the synthesis gas test bench and in long-term engine tests when varying engine-specific parameters, conducted on a single cylinder dual-fuel marine engine. For these investigations, the center of combustion, the air-fuel equivalence ratio, the flow rate and the space velocity were varied and the conversion rate was comprehensively investigated. The extensive investigations in this paper on the synthetic gas test bench and also single cylinder research engine provide an overview of the extent to which an MOC with palladium coating is suitable as a simple retrofit solution for reducing green house gas emissions from dual-fuel marine engines. If a retrofit solution is practical, there is potential for cost savings through the EU Emission Trading System and those induced by the penalties which are to be introduced by the IMO.

1 INTRODUCTION

The number of ships powered by LNG (liquefied natural gas) engines is steadily increasing [1]. There are many reasons for the popularity of lean-burn gas engines. On the one hand, these engines have already been tried and tested many times, are reliable for shipowners and also economically comparable to MGO (marine gas oil) [2]. On the other hand, an operation with LNG reduces emissions in comparison to diesel engine operation, especially reducing particulate matter and nitrogen oxides relevant to the IMO (International Maritime Organisation) [3].

The composition of natural gas varies worldwide, with the main component of natural gas being methane [4]. The alkane methane has the most favourable C-H ratio and theoretically emits around 25 % less CO_2 during combustion than a conventional diesel fuel. In addition, almost no particulate emissions are formed. By reducing nitrogen oxides, the conversion to LNG engines represents an opportunity to operate the ship in compliance with IMO TIER III even without exhaust gas aftertreatment [5].

A disadvantage to be mentioned is the methane slip that exists in LNG engines. With methane slip, the fuel gas - mainly methane - escapes unburnt from the cylinder. In addition to a reduction in efficiency, this has ecological consequences. With a GWP (Global warming potential) Factor of 29.8 over 100 years, methane has a significant impact on the climate [6]. The avoidance of unburnt methane is therefore immensely important when using LNG engines.

The methane slip of different LNG engine types is quantified in Table 1. A distinction is made here between spark-ignited LBSI (Lean-burn spark ignited) engines and medium-speed 4-stroke LPDF (Low pressure dual-fuel) engines ignited with a diesel pilot, as well as low-speed 2-stroke LPDF and HPDF (High pressure dual-fuel) engines. The slow-running 2-strokes, which are often used to power LNG carriers and container ships have the most favourable level of methane slip. The LBSI engine has a high methane slip of 4.1 g/kWh, but due to the lack of a diesel fallback level, it does not have a high market penetration. The medium-speed 4-stroke LPDF has the highest methane slip, and also has the highest market penetration of the engine types shown here. The investigations in this paper were carried out on this engine type.

Table 1. Methane-slip of different marine engine types [7].

Engine type	Example ship types	CH_4-slip
Unit		g/kWh
LBSI, medium-speed	Car / passenger ferries (e.g. Rolls-Royce/ Bergen C26:33L9PG	4.1
LPDF, medium-speed, four-stroke	LNG carriers (e. g. Wärtsilä 12V50DF); LNG-fueled cruise ships (e.g. MaK 16M46DF)	5.5
LPDF, slow-speed, two stroke	container ships (e. g. Wärtsilä/WinGD 12X92DF)	2.5
HPDF, slow-speed, two-stroke	LNG carriers (e.g. Man_B&W 5G70ME-C9-GI)	0.2

The causes of methane slip in LPDF engines with a PFI (port fuel injection) system are scavenging losses in turbocharged engines and the escape of unburnt CH_4 through flame quenching on cold cylinder walls or crevices within the cylinder, for example above the 1st piston ring. Flame quenching on the cylinder walls is dominant over the entire power band of the engine [8]. Due to the high market penetration of LPDF engines and the existing methane slip of these, post-engine solutions can be a key to reducing CH_4 emissions.

Methane oxidation catalysts (MOC) are one option for post-engine methane slip reduction. In catalytic oxidation, the exhaust gas flow is usually channeled through materials containing precious metals - e.g., Palladium (Pd) in this paper. The oxidation of CH_4 is shown in equation (1) [9].

$$CH_4 + 2O_2 \rightarrow CO_2 + H_2O,\ \Delta H^0 = -803\ kJ\ mol^{-1} \quad (1)$$

The advantage of Pd-containing catalysts is the high conversion rate of methane at lower temperatures. Pd-containing catalysts are therefore described in literature as the most suitable for engines in lean operation in order to achieve the high bond dissociation enthalpy of 440 kJ/mol for splitting the molecules [10].

In this paper, various variations are carried out on an MOC. The inhibiting influence of NO and CO_2 is determined on the synthesis gas test bench. In addition, the tests on the single-cylinder engine are intended to show what influence can be exerted on the MOC from an engine perspective. The deactivation behaviour of the MOC after just over 30 operating hours will also be demonstrated in order to assess its suitability.

2 EXPERIMENTAL SETUP

The following describes the setup of the synthetic gas test bench as well as the single-cylinder test bench.

2.1 Synthetic gas test bench

The synthetic gas test bench at the University of Rostock offers the possibility of testing a wide variety of catalysts in an isothermal environment under defined conditions. An overview of the test bench is shown in Figure 1.

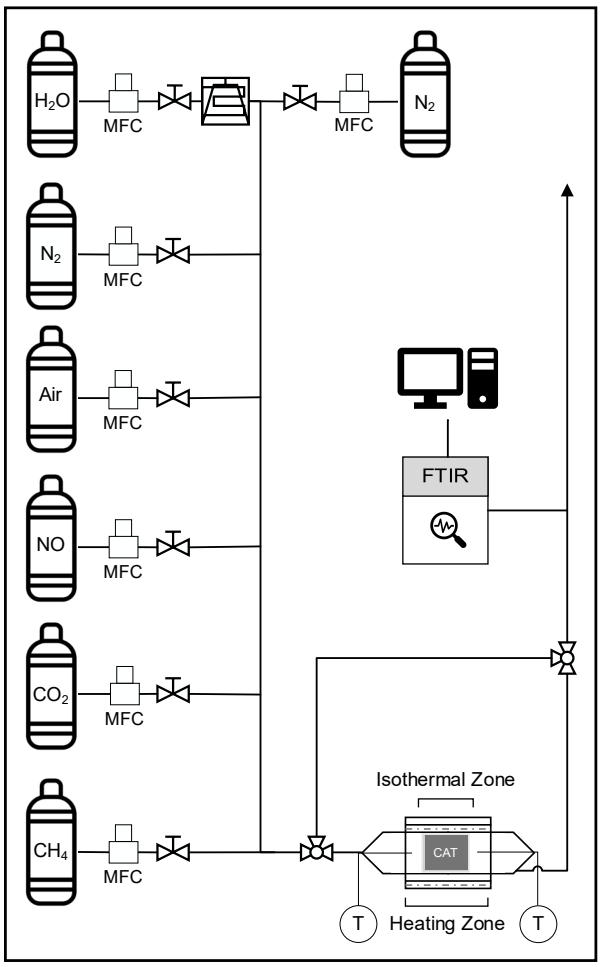

Figure 1. Overview of the Synthesis gas test bench

The various test gases are transported from the pressurised gas cylinders into an insulated gas pipe heated to 100 °C and fed to the catalytic converter test bench (shown in Figure 1 as “CAT”). A vaporisation unit ensures that the water is completely vaporised. The test gas mass flow is controlled by mass flow controllers (MFC). The test gas mixture can then be channeled directly to the Fourier transform infrared (FTIR) spectroscope or to the catalytic converter test rig using a distribution valve. Using this distribution valve, the raw test gas can be compared with the gas mixture after the catalyst. The catalytic converter test rig can be heated from 100 °C to up to 600 °C and the temperature and speed of the temperature change can be changed individually. The temperature is controlled by type K thermocouples. The temperature increase resulting from the exothermic catalyst reaction can be observed using temperature measurements. The FTIR measuring device is located downstream of the catalytic converter test rig.

2.2 Single cylinder test bench

With the 1/34 DF single-cylinder engine, the Department of Piston Machines and internal Combustion Engines (LKV) at the University of Rostock has the opportunity to carry out engine tests on one of the largest research engines at a European university. The engine has a bore of 340 mm and a stroke of 460 mm, making it ideal for research into marine engines. The test bench was set up in 2014 and has been successively expanded. The engine has the following characteristics and capabilities as shown in Figure 2:

- Pilot fuel system up to 2,200 bar
- Gas mixing unit: natural gas, CO_2, H_2, C_3H_8
- NGC (Natural Gas Chromatograph) for gas quality assessment
- HP (High Pressure) gas supply up to 600 bar
- Methanol & LPG supply possible
- Charge air supply up to 8.5 bar(a)
- Charge air heating & humidification
- Open Engine control unit (ECU) platform
- FTIR with 2 lines for exhaust analysis
- Exhaust gas recirculating-System allowing rates up to 30 % at full load
- Bypass for exhaust gas aftertreatment components

Two of the test bed’s features were decisive in the creation of the presented findings and shall be further expanded upon here: The research ECU and the bypass for exhaust gas aftertreatment components. The engine is equipped with a freely programmable research ECU based on the PXI platform by National Instruments. It is also possible to perform an online pressure indication and the necessary thermodynamic analysis for next cycle control strategies. The control parameters are as followed:

- Pilot Start of Injection (SOI_{Pilot})
- Pilot duration
- Pilot Rail pressure
- SOGAV (Solenoid operated gas admission valve) Start of Injection (SOI_{SOGAV})
- SOGAV duration
- Center of combustion (CoC_{50})
- Indicated mean pressure (p_{mi})

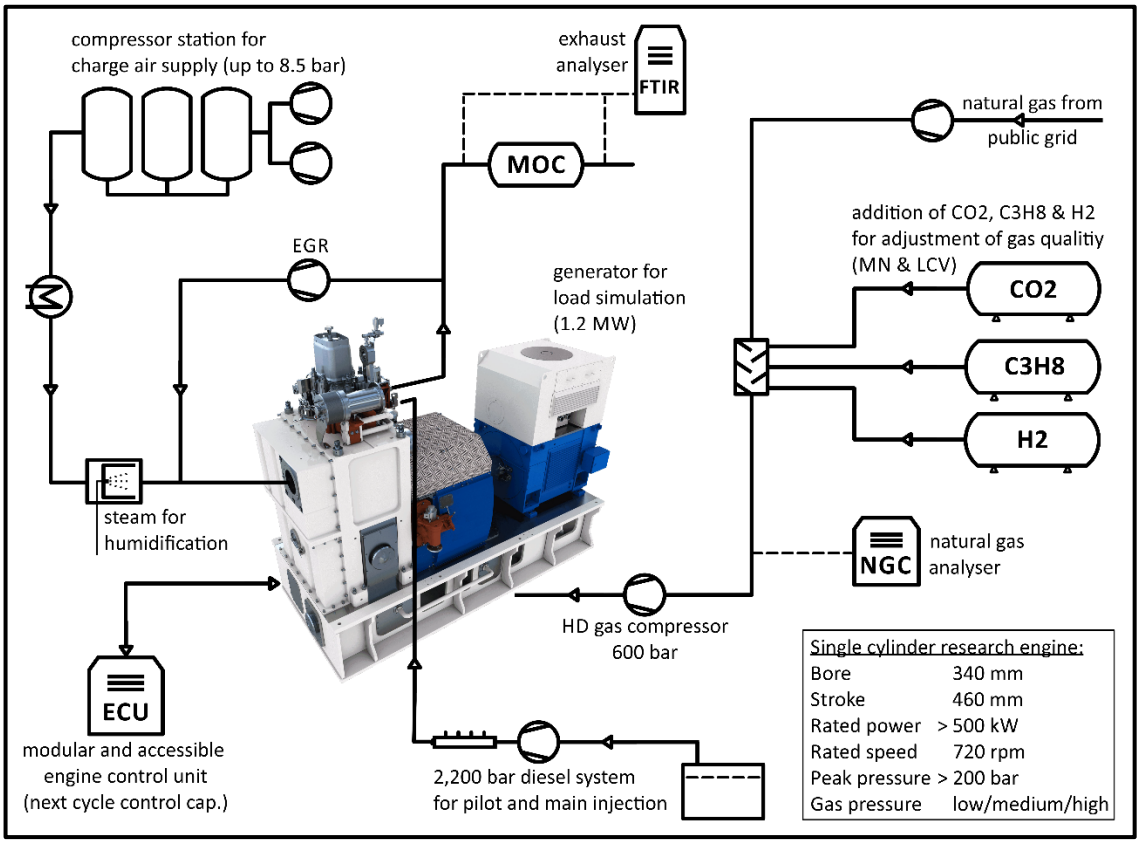

Figure 2: Diagram of the used experimental engine testbed-infrastructure

The bypass for analysing the exhaust gas aftertreatment components was set up as part of the TEME2030+ project. The schematic is shown in Figure 3. The DN150 exhaust gas path, which was used to control the exhaust gas back pressure to simulate an exhaust gas turbocharger, was extended by a DN50 pipe. In addition, it was possible to measure with a SESAM i60 FTIR measuring device on two lines and thus check the exhaust gas measurement values before and after the catalytic converter.

After the DN50 electric control valve, an MOC housing for the catalyst was installed in which a total of two catalytic converters connected in series with the standard dimensions of 150 mm x 150 mm x 150 mm fit (shown as “CAT”). A further control valve is located downstream in order to vary the gas pressure to change the gas density. The bypass section is equipped with various temperature and pressure sensors.

The existing exhaust gas measuring section was also extended. Originally, the exhaust gas was extracted from the manifold and routed to the FTIR measuring device via a heated pipe. For the investigations carried out in this paper, a sampling unit was set up to switch the extraction between the exhaust gas measuring points in the manifold, before the catalytic converter and after the catalytic

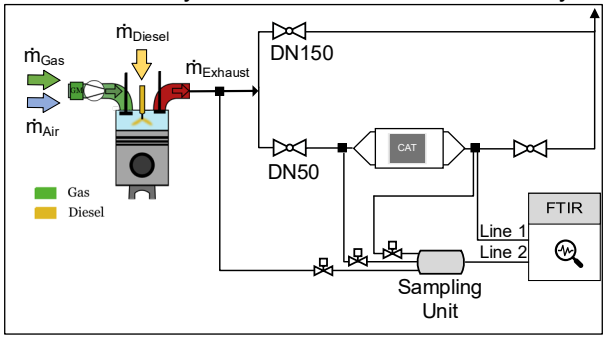

Figure 3. Bypass route for analysing exhaust gas aftertreatment components

converter, using solenoid valves and to route it to line 2 of the FTIR. There is also a connection between the extraction position after the catalytic converter and line 1 of the FTIR. This modification makes it possible to measure the emissions upstream and downstream of the catalytic converter in parallel, to validate the measurement accuracy by means of a parallel measurement and also to carry out standard sampling from the manifold.

The PFI low-pressure combustion process of the engine uses a SOGAV in the intake manifold. This combustion process is frequently used in the field due to its simple design and low operating pressures. The pilot injector is located in the cylinder head and provides the diesel ignition. The engine is operated on the generator curve at 720 min^{-1} and is therefore representative for medium-speed marine engines. The entire engine infrastructure shown in Figure 2 is monitored and controlled by a programmable logic controller (PLC), the measured values are recorded at 1 Hz for 140 s and then averaged. High-frequency measurements such as cylinder pressure or the rate of heat release (RoHR) and the associated determination of the CoC are recorded with a resolution of 0.1 °CA (degrees crank angle) and averaged over 250 cycles.

2.3 Palladium-Catalyst

The properties of the catalyst used are shown in Table 2.

Table 2: Catalyst Properties

Property	Value	Unit
Size	150 x 150 x 150	mm
Number of cells	100	cpsi
Volume	3.375	l
Substrate	Ceramic (cordierite)	-
Coating	Pd/Al_20_3	-
Pd-concentration	2.2	g/l

3 METHODS

The methodology of the results shown in this paper allows for a basic measurement of the Pd-catalyst on the synthesis gas test bench. In addition, the inhibiting effect of some substances on the catalyst is investigated. The catalytic converter is then installed in the bypass section described in Chapter 2.2 on the single-cylinder test bench and its performance is analysed under different engine operating variations.

3.1 Synthetic gas test bench

The tests on the synthetic gas test bench are used to determine the light-off temperature and to visualise the maximum conversion rate when varying gas compositions are added. A temperature ramp of 5 K/min is used to measure these variations. The tests start at a temperature of 250 °C and end at 500 °C. This temperature is then maintained for approximately one hour and the MOC is exposed to the test gas before the temperature is gradually reduced to 250 °C again. Typically, there is a hysteresis effect between the heating and cooling curves, i.e., different conversion rates at the respective temperatures.

3.1.1 Catalyst Sample

A catalyst sample of the catalyst described in section 2.3 was prepared for the synthetic gas tests. A cylindrical core sample with a diameter of 25.4 mm and a length of 50.8 mm was taken. The sample has 76 channels. The tests are carried out with this sample at a standardized gas hourly space velocity (GHSV) of 50,000 h^{-1}. The calculation of the GHSV is shown in Formula 2

$$GHSV = \frac{\dot{V}_{MOC}}{V_{MOC}} \quad (2)$$

with $\dot{V}_{MOC}$ the volumetric flow rate, and V_{MOC} the volume of the catalyst. The conditions according to ISO6358 / ISO8778 are 1 bar atmospheric pressure and 20 °C. These values were used for the calculation of the standard volume flow.

3.1.2 Variations

The variations are used for general catalyst characterisation, starting with a basic measurement with CH_4 and O_2. The inhibiting influences of NO and CO_2 are then analysed. The influence of NO on the Pd catalyst is described differently in the available literature. For example, Auvinen et al. report a detrimental effect of NO when added to the test gas in a fresh Pd-MOC due to site blocking and competition for active sites due to strong adsorption by NO [11]. However, in the case of poisoning by sulphur dioxide, the addition of NO promotes methane oxidation. Sadokhina et al. investigated the effect of NO in the presence of a wet feed. The authors report a blocking effect of NO, but only with dry exhaust gas and a promoting effect with wet exhaust gas [3]. Hurtado could not recognise any noticeable effect with the addition of NO [12].

The measurement matrix for the synthesis gas test rig is shown in Table 3. This paper analyses the influence of 250 ppm NO and 7.9 vol.% CO_2. In every mixture, N_2 balances the testing gas to fulfill the standard GHSV.

Table 3: Measurement matrix synthesis gas test bench

Mixture	Basic	Basic + NO	Basic + NO + CO_2
CH_4	1050 ppm	1050 ppm	1050 ppm
O_2	7.9 %	7.9 %	7.9 %
NO	-	250 ppm	250 ppm
CO_2	-		7.9 %
N_2	as required	as required	as required

The inhibitory effect of SO_2 and H_2O has already been intensively investigated and described. It has been reported that poisoning of the MOC begins at 1 ppm SO_2 in the test gas and that a higher addition accelerates the poisoning disproportionately [13]. Accelerated deactivation due to H_2O has also been reported [14]. Due to these known deactivation effects, the two gases were not added to the test gas during the tests.

3.2 Single cylinder test bench

After the tests on the synthesis gas test rig, the catalytic converter was tested in extensive engine tests. The focus here is on the conversion rate of the catalytic converter under changing engine operation and the durability of the catalytic converter under real conditions.

The tests on the single-cylinder test bench were carried out at a mean pressure of 10.8 bar, which corresponds to a 50 % load point. The rail pressure of the common rail diesel system is 1200 bar, the gas pressure 3.55 bar(a). The pilot quantity for the tests is 60 mg/shot. The charge air is preheated to 45 °C to create constant conditions. In order to ensure increased methane emissions with a simultaneously increased exhaust gas temperature, a late centre of combustion (CoC) of 10 °CAaTDC (degrees crank angle after top dead center) was selected for the tests. An overview of the engine settings is shown in Table 4.

Table 4: Engine operating point

Parameter	Symbol	Value	Unit
Speed	n	720	min^{-1}
Load	-	50	%
IMEP	p_{mi}	10.8	bar
Diesel pressure	p_{Rail}	1200	bar
Gas pressure	p_{Gas}	3.55	bar(a)
Diesel quantity	m_{Pilot}	60	mg/shot
Charge air presssure	p_{Air}	2.05	bar
Exhaust gas pressure	p_{Exh}	1.75	bar
Air temperature	T_{LL}	45	°C
CoC	α_{50}	10	°CA aTDC
Bypass pressure	p_{CAT}	1.2	bar
GHSV	v_R	60000	h^{-1}

On the one hand, the engine settings are used to ensure constant engine conditions for the different variations. In addition, the engine operating point described in Table 4 is used as a reference point to determine the CAT deactivation. The exhaust gas composition at the reference point is as follows:

Table 5: Exhaust gas components at the MOC reference points

Exhaust gas component	Value	Unit
O_2	11	Vol.%
H_2O	10	Vol.%
CO_2	5	Vol.%
CH_4	700	ppm
NO	60	ppm

The engine exhaust gas consists of 11 vol.% O_2, 10 vol.% H_2O and around 5 vol.% CO_2. The exhaust gas also contains around 700 ppm CH_4 and 60 ppm NO. Due to the sulphur-free fuel, the SO_2 values are negligible.

Different variations are carried out for MOC testing. The measurement matrix for the single-cylinder engine test bench is shown in Table 6.

Table 6: Variations on the engine test bed

No.	Variation	Investigation
1	Heating Up	CH_4 Conversion by temperature
2	CoC	Influence of temperature increase
3	Air Ratio	Influence of increasing water content
4	Pressure	Influence of flow velocity
5	Mass Flow	Influence of GHSV
6	Reference	Deactivation determination

The engine is warmed up at the start of the tests. As soon as a stable operating temperature has been reached, the bypass was opened for the MOC tests in order to heat it up and determine the light-off temperature. The reference point is then approached. This reference point is approached at regular intervals during the tests in order to determine the CH_4 conversion rate and thus the deactivation of the catalytic converter. The first variation deals with the influence of the temperature by changing the CoC. The lambda variation is used to analyse the influence of the water content in the exhaust gas. Water has, as described, a damaging effect on the MOC. Test number 4 deals with the variation of the flow velocity due to a change in pressure and the associated change in density of the exhaust gas. Here, the exhaust gas pressure acting on the catalytic converter is varied from 1.2 bar to 1.6 bar using the exhaust gas flap downstream of the catalyst. Variation No. 5 is a variation of the standardized GHSV by increasing the mass flow through the bypass. It is important to mention here

that an isolated observation of effects is not possible in the engine tests, as cross-influences occur. Variation 2 can be cited as an example here, in which a later CoC increases methane emissions, while also increasing the exhaust gas temperature, which has a positive effect on the methane conversion of the catalytic converter.

4 RESULTS

4.1 Synthesis gas test rig

Figure 4 shows the CH_4 conversion rate of the various test gases while the temperature is ramped up or down. The light-off temperature of the MOC can be read from this diagram, whereby a distinction can be made between the heating and cooling phases.

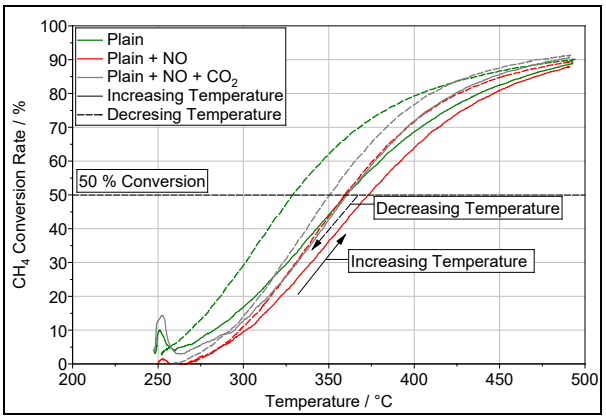

Figure 4. Determination of the Light-Off temperature

It is clear to see that the mentioned hysteresis effects occur. This can be recognised by the higher conversion rates of the test gases in the cooling curves. In the heating tests, almost no difference is recognisable in the lower temperature field for the three test gases. CH_4 conversion begins at around 275 °C for all gases. Subsequently, the adsorption of NO on the PdO formed has a negative influence on the conversion rate, as already described by [11]. However, this influence appears to be reversed from temperatures > 400 °C, as the conversion rates then gradually approach the rates of the test gas with CH_4 and O_2 again. When CO_2 is added to the test gas, a delayed CH_4 conversion can be observed. From approx. 375 °C, however, the addition of CO_2 to the test gas causes an improvement in the conversion rate. This test gas achieves the highest conversion rate of 91 %. The light-off temperatures are 360 °C and 370°C respectively.

In addition, the catalyst sample was exposed to the test gas for one hour after heating to 500° C. This test is shown in Figure 5. The test gas in which NO was added has the lowest conversion rate. The test gas with CH_4 and O_2 performs about one percentage point better. The positive influence of CO_2 is also recognisable here. No deactivation effects occur after one hour of operation at 500 °C. Deactivation effects can occur even without the addition of water to the test gas and blocking by the hydroxyl groups, as water is formed during the oxidation of CH_4 [10].

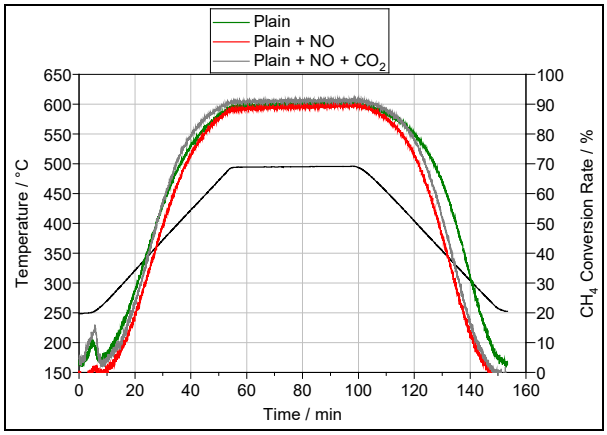

Figure 5. CH4 Conversion Rate of the test gases

4.2 Single cylinder test bench

The results achieved on the single-cylinder test bench are shown below. The sequence of the variations corresponds to the measurement matrix in Table 6. It is important to note here that, for reasons of practicability, this sequence does not correspond to that of the actual test runs. As a result, some of the conversion rates of some variations are lower on average than others, as these were run chronologically later and the MOC already shows deactivation effects.

4.2.1 Heating behaviour

Figure 6 shows the heating behaviour of the MOC. The grey line shows the temperature at the exhaust manifold. The constant temperature indicates that the engine is fully warmed up when the bypass flap is opened and a static engine operating point is present. The temperature upstream of the MOC (red line) rises to 300 °C within a few minutes, at which point the CH_4 conversion starts. The light-off temperature is reached after around 11 minutes and is around 400 °C. From around 420 °C, the exothermic methane oxidation can also be observed in a temperature increase after the MOC. The absolute emissions of CH_4 fall from around 900 ppm to around 100 ppm when the final temperature in front of the MOC of around 475 °C is reached. This represents a conversion rate of almost 90 % and is slightly below the conversion rates achieved on the synthesis gas test rig.

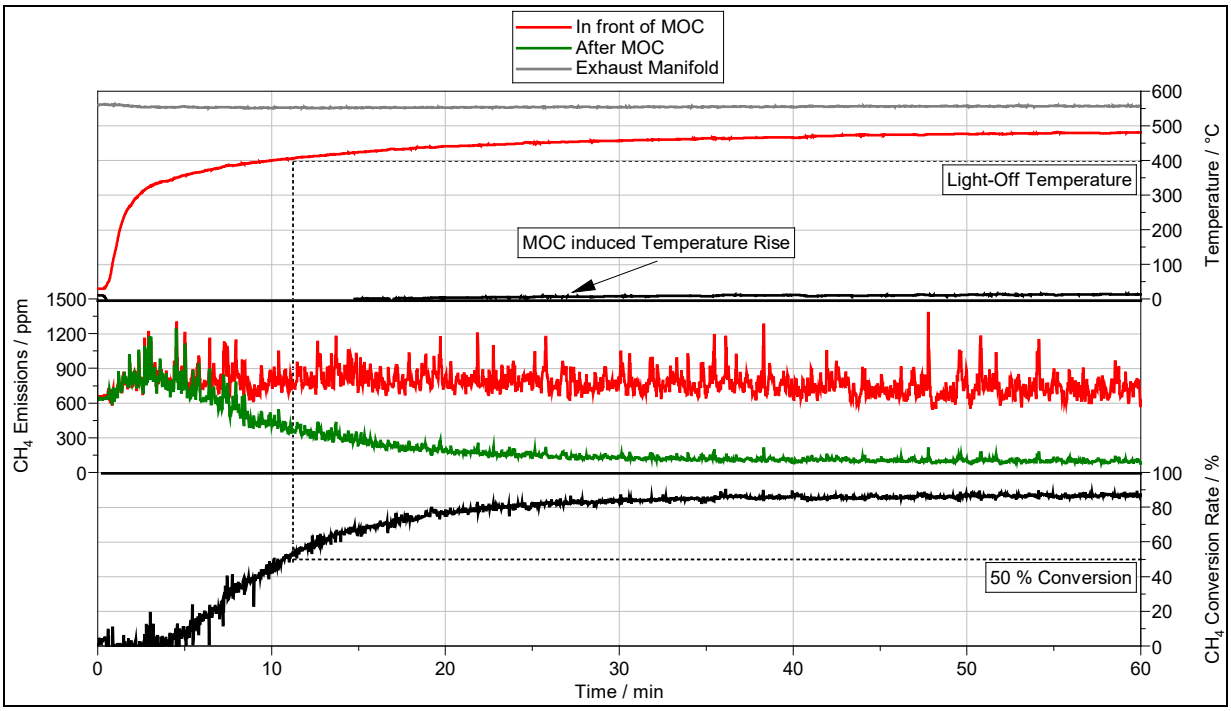

Figure 6. Determination of the Light-Off temperature at the single-cylinder research engine

4.2.2 CoC Variation

The variation of the CoC is shown in Figure 7. The late CoC reduces the efficiency, which also causes a temperature increase in the manifold or in front of the MOC. The temperature in front of the MOC rises from 485 °C to 517 °C; a temperature increase of around 32 °C. However, the late CoC also causes other changes. In addition to the air/fuel ratio lambda, the conditions in the bypass section also change. The change in the CoC causes an increasing exhaust gas and bypass mass flow due to adjusting the DN50 exhaust valve to keep the exhaust gas pressure stable for the simulation of the exhaust gas turbocharger. The rise in temperature also increases the volume flow, which can be observed in a higher flow velocity through the bypass. By increasing the bypass mass flow rate, the normalised GHSV also increases gradually from around 57,000 h^{-1} to 64,000 h^{-1}. Nevertheless, the temperature dependence of the MOC already shown in the synthetic gas experiments can be recognised in this variation. Despite increasing CH_4 emissions at a later CoC and higher GHSV, the CH_4 conversion rate increases from 68 % to 76 %, which corresponds to an increase of around 11.8 %.

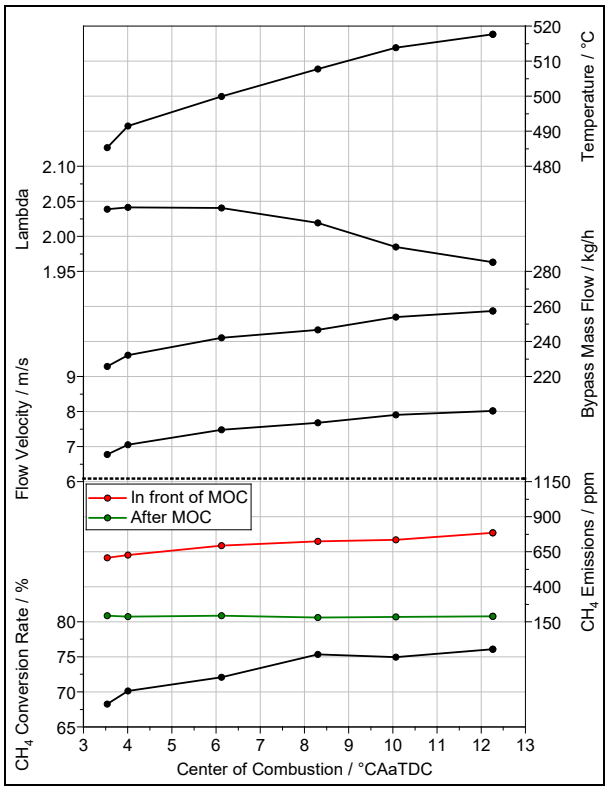

Figure 7. CH_4 Conversion by varying the CoC50

4.2.3 Lambda variation

A reduced lambda increases the water content in the engine exhaust. This variation is shown in Figure 8 . The lambda values vary from 1.78 to 2.12. A positive aspect of this variation is that the standardized GHSV can be kept almost constant. The water content in the exhaust gas falls from around 12.3 vol.% to 9.8 vol.%. With this variation, the exhaust gas temperature is particularly influenced. As with the previous variation, the temperature difference is around 35 °C. In addition, the CO_2 emissions, which had a positive effect on the conversion rate in the synthesis gas tests, also decrease. These influences result in a slight decrease in the CH_4 conversion rate.

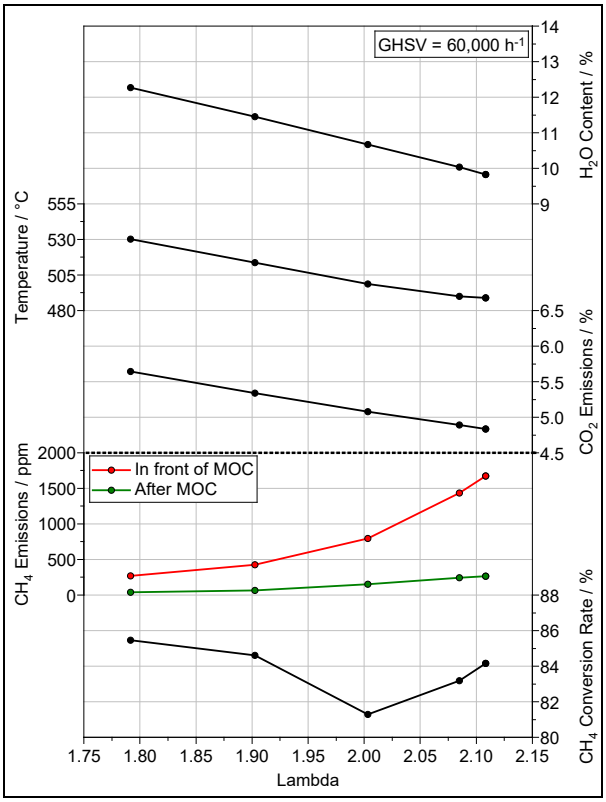

Figure 8. CH4 Conversion by changing the air/fuel Ratio

4.2.4 Pressure Variation

The pressure variation shown in Figure 9 was carried out within the limits of 1.2 bar to 1.6 bar. As the exhaust back pressure is 1.75 bar, a variation was only possible within these limits. As described, this variation has an influence on the exhaust gas density in the bypass section and therefore the flow velocity through the MOC varies. Apart from the volumetric change, however, the influence of this variation can be analysed in isolation without cross-influence. The conversion rate increases only marginally at low flow velocities, so that an influence cannot be recognised.

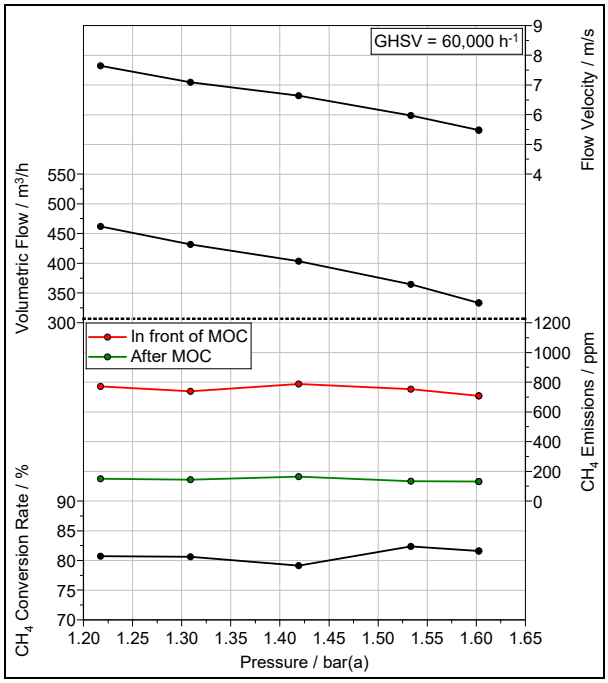

Figure 9. CH4 Conversion by changing Bypass pressure

4.2.5 Bypass Mass Flow Variation

Figure 10 shows the flow variation, which also represents a change in the standardized GHSV.

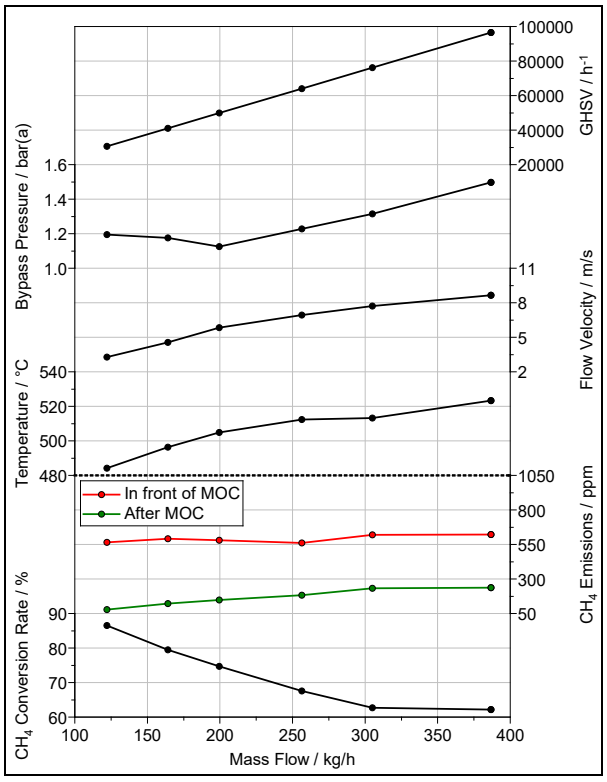

Figure 10. CH4 Conversion with varying Mass Flow

With this variation, the standardised GHSV can be increased from 30,000 h^{-1} to up to 96,000 h^{-1}. In addition to the increase in the GHSV, the increase in mass flow through the bypass section also results in an pressure-increase in the bypass. The real volume flow also increases due to the higher mass flow and the rise in temperature, which results in an increase in the flow velocity through the catalytic converter. In addition, the increase in the hot exhaust gas mass flow also raises the temperature upstream of the MOC by 38 °C to 523 °C and thus corresponds approximately to the values from chapter 4.2.2. Despite the temperature increase, a deterioration in the CH_4 conversion is clearly recognisable. The increase in the GHSV from 30,000 h^{-1} to 96,000 h^{-1} results in the conversion rate falling from around 87 % to around 62 %. This corresponds to a decrease of almost 29 %. The influence of the GHSV is therefore clearly recognisable.

4.2.6 Reference Points

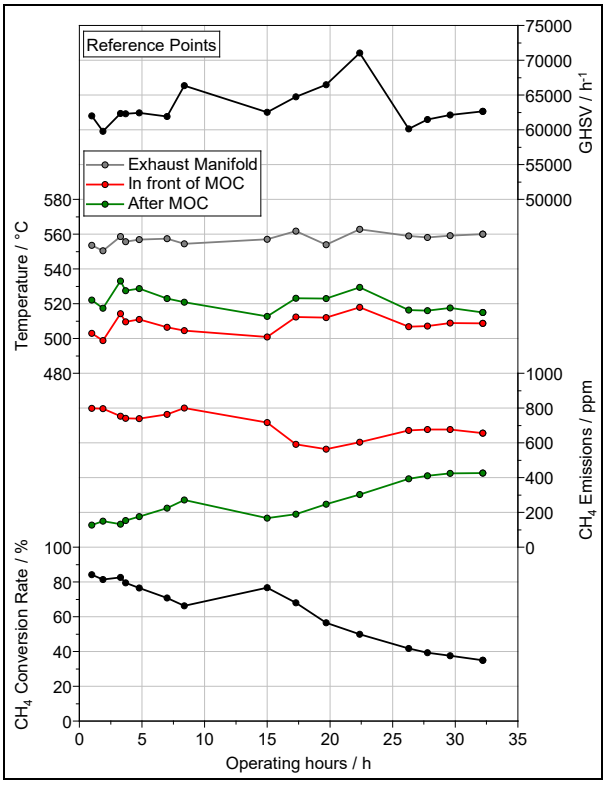

Figure 11. Deactivation of the MOC

A reference point was used to determine the deactivation of the MOC. As seen in Figure 11, the reference point was approached 15 times between the above-mentioned parameter variations. The GHSV was slightly above 60000 h^{-1} during the measurements, and the temperatures were around 510 °C in front of the MOC for all measurements. The ever-decreasing temperature difference between the measuring points before and after the MOC indicates that the exothermic reactions are decreasing and less CH_4 is being converted. The conversion rate of the MOC drops from 85 % to 35 % after just over 32 operating hours. This corresponds to a deactivation of the MOC of 59 %. The increase in the conversion rate after the 7th measuring point, or after around 7.8 operating hours, is also of interest. This measuring point represents the end of a measuring day. On the following measurement day, at the 8th reference point, a slight regeneration apparently took place, which was not repeated on the following measurement days. The bypass route was flushed with air after each measurement.

5 CONCLUSIONS

The importance of LNG engines in shipping is high and capacities will be further expanded in the future due to the demand for ever cleaner transport options. LNG can already make a contribution to the maritime energy transition by using blends of climate-neutral bio-LNG or syn-LNG. The harmful methane slip cancels out the CO_2 advantage, as up to 5.5 g/kWh of CH_4 is emitted depending on the type of ship, meaning that these emissions must be reduced either by improving combustion (see also Paper No. 105) and reducing methane slip during valve overlap (see also Paper No. 156) or by adequate exhaust gas aftertreatment.

One possibility is the Pd/Al_2O_3-MOC presented in this paper, which promises high CH_4 conversion rates without the need for an external heating module. Various measures were taken as part of the paper to evaluate its suitability for series operation. For example, the synthetic gas test bench at the University of Rostock was used for basic measurement. For this purpose, a cylindrical core sample was prepared in order to determine the CH_4 conversion rates and thus the light-off temperatures by means of a defined temperature increase or decrease at a GHSV of 50,000 h^{-1}. The MOC was measured using a CH_4-O_2 mixture, and the inhibitory effects of NO and CO_2 were also examined.

The University's single-cylinder engine test bench was modified for the evaluation of the MOC in an engine. On the one hand, the existing exhaust gas extraction and measurement system was modified and, on the other, the existing exhaust tract was rebuilt. The exhaust gas measurement with the Sesam i60 FTIR was modified so that emissions can now be measured in parallel before and after the MOC. In addition, the parallel measurement at the same measuring point made it possible to check the comparability of both exhaust gas lines. In order to test the MOC brick, the existing exhaust gas path was extended. Originally, the exhaust gas was discharged via a DN150 exhaust gas path with

a throttle valve. This path was extended by a DN50 exhaust gas path with the option of connecting two consecutive MOCs in series to further reduce the GHSV. The pressure in the bypass can be varied using two throttle valves. With these modifications, the MOC behavior can be investigated by varying various parameters.

The tests on the synthetic gas test bench showed that the addition of NO or CO_2 to the test gas has an influence. While NO tends to reduce the conversion rate due to adsorption, CO_2 has a positive influence. The influence of water or SO_2 on the deactivation behavior is already well described and was not investigated in this paper.

Variations were carried out during the test bench trials in order to investigate possible influences on the CH_4 conversion rate. For example, the heating behavior was investigated to determine the light-off temperature of the MOC during the engine tests. The engine CoC and lambda were varied under constant conditions in the MOC bypass. In addition to the engine tests, the exhaust gas pressure was varied in the MOC bypass by varying the exhaust gas flap position and the influence of varying the GHSV was investigated. Finally, a recording of reference points was used to quantitatively determine the deactivation of the MOC after the respective operating time.

The tests showed that the light-off temperature in the engine tests was slightly higher than the light-off temperature in the synthesis gas tests. This is presumably due to lateral influences from other exhaust gas components. From an engine point of view, a late center of combustion is beneficial, as this increases the temperatures in the exhaust tract. On the downside, however, it should be mentioned that such a late center of combustion has disadvantages in terms of efficiency and high CH_4 values. A low GHSV should be selected in the bypass. There is a trade-off here, as the MOC cannot be infinitely large due to the lack of space. GHSW values < 50,000 h^{-1} are advisable when dimensioning the MOC. One way to reduce the GHSV is to connect the MOC in series. The lambda and pressure variation did not affect the CH_4 Conversion of the MOC. The reference points showed that the MOC has a deactivation rate of around 59 % after 32 operating hours. This value was achieved without possible regeneration strategies.

The results shown confirm that high CH_4 conversion rates are possible with a Pd/Al_2O_3 MOC applied to lean-burn natural gas engines operating even at low temperatures. Nevertheless, the catalyst exhibited a 50 % performance loss after only 26 operating hours, which represents a longer service life than described in some of the literature [13]. However, such a deactivation would be fatal for the ship owner. It would therefore be important to develop realistic regeneration concepts for an onboard regeneration. One regeneration possibility is for example multiple short CH_4 pulses in front of the MOC [15], [16]. If the long-term stability of the mixture is further improved, or an adequate regeneration strategy exists that is easy for the shipowner to implement, the Pd/Al_2O_3 MOC could prove an effective way to reduce methane emissions post-engine.

6 DEFINITIONS, ACRONYMS, ABBREVIATIONS

°CA	Degrees crank angle
°CAaTDC	Degrees crank angle after top dead center
CH_4	Methane
CO_2	Carbon dioxide
CoC	Center of combustion
ECU	Engine control unit
FTIR	Fourier Transform Infrared Spectroscopy
GWP	Global warming potential
GHSV	Gas hourly space velocity (Standardized)
H_2O	Water
HPDF	High pressure dual-fuel
IMEP	Indicated mean effective pressure
IMO	International Maritime Organisation
ISO	International Organization for Standardization
LBSI	Lean-burn spark ignited
LKV	Department Piston Machines and internal Combustion Engines
LNG	Liquefied natural gas
LPDF	Low pressure dual-fuel
MFC	Mass flow controller

MGO	Marine gas oil
MOC	Methane oxidation catalyst
NO	Nitrogen monoxide
O_2	Oxygen
Pd	Palladium
PFI	Port fuel injection
PLC	Programmable logic controller
ppm	Parts per million
RoHR	Rate of heat release
SOI	Start of injection
SOGAV	Solenoid operated gas admission valve

7 ACKNOWLEDGMENTS

The authors would like to thank the German Federal Ministry for Economic Affairs and Climate Actions for funding the project TEME2030+ (project number: 03SX537C). Furthermore, our thanks go to FVTR GmbH, Schaller Automation GmbH & Co. KG, Umicore AG & Co. KG, Kolbenschmidt GmbH, Kompressorenbau Bannewitz GmbH, Sick AG and M. Jürgensen GmbH & Co KG for supporting these projects.

8 REFERENCES AND BIBLIOGRAPHY

[1] DNV, 2024. Maritime Forecast to 2050 – Energy Transition Outlook 2024

[2] Bilgili, L. 2023. A systematic review on the acceptance of alternative fuels, *Renewable and Sustainable Energy Reviews,* 182: 113367.

[3] Sadokhina, N. et al. 2017. The influence of gas composition on Pd-based catalyst activity in methane oxidation − inhibition and promotion by NO, *Applied Catalysis B: Environmental,* 200: 351-360.

[4] Schleef, K. 2024. Analyse und Optimierung des Verbrennungsprozesses von Dual-Fuel-Motoren bei Betrieb mit schwankenden Brenngasqualitäten, phd thesis, University of Rostock.

[5] Ushakov, S. et al. 2019. Methane slip from gas fuelled ships: a comprehensive summary based on measurement data, *Journal of Marine Science and Technology*, 24: 1308-1325.

[6] IPCC, 2024. IPCC Global Warming Potential Values – Updated AR6 values

[7] Pavlenko, N., Comer, B., Zhou, Y., Clark, N., Rutherford, D., 2020, The climate implications of using LNG as a marine fuel, *working paper 2020-02*, ICCT.

[8] Jensen, M.V. et al. 2021. Numerical analysis of methane slip source distribution in a four-stroke dual-fuel marine engine, *Journal of Marine Science and Technology*, 26: 606-617.

[9] Chen, W.H and Lin, S.C. 2016. Characterization of catalytic partial oxidation of methane with carbon dioxide utilization and excess enthalpy recovery, *Applied Energy*, 162: 1141-1152.

[10] Lott, P. et al. 2024. A review on exhaust gas after-treatment of lean-burn natural gas engines – From fundamentals to application, *Applied Catalysis B: Environmental*, 340: 123241.

[11] Auvinen, P. et al. 2021. Effects of NO and NO2 on fresh and SO2 poisoned methane oxidation catalyst – Harmful or beneficial?, *Chemical Engineering Journal,* 417: 128050.

[12] Hurtado, P. et al. 2004. Combustion of methane over palladium catalyst in the presence of inorganic compounds: inhibition and deactivation phenomena, *Applied Catalysis B: Environmental*, 47: 85-93.

[13] Ottinger, N. et al. 2015. Desulfation of Pd-based Oxidation Catalysts for Lean-burn Natural Gas and Dual-fuel Applications, *SAE International Journal of Engines*, 8(4): 1472-1477.

[14] Persson, K. et al. 2007. Stability of palladium-based catalysts during catalytic combustion of methane: The influence of water, *Applied Cataysis B: Environmental*, 74 (3-4): 242-250.

[15] Arosio, F. et al. 2006. Regeneration of S-poisoned Pd/Al2O3 catalysts for the combustion of methane, *Catalysis Today*, 117(4): 569-576.

[16] Honkanen, M. et al. 2018. Regeneration of sulfur-poisoned Pd-based catalyst for natural gas oxidation, *Journal of Catalysis*, 358: 253-265.

9 CONTACT

Pascal Seipel, University of Rostock

Mail: pascal.seipel@uni-rostock.de

Web: www.lkv.uni-rostock.de
www.teme2030.de